Received: 23 April 2018 | Revised: 14 September 2018 | Accepted: 16 October 2018

DOI: 10.1002/hbm.24446

WILEY

RESEARCH ARTICLE

Social decision-making in the brain: Input-state-output modelling reveals patterns of effective connectivity underlying reciprocal choices

Daniel Shaw[1,2] | Kristína Czekóová[2] | Martin Gajdoš[3] | Rostislav Staněk[4] | Jiří Špalek[5] | Milan Brázdil[2]

[1]Department of Psychology, School of Life and Health Sciences, Aston University, Birmingham, United Kingdom

[2]Behavioural and Social Neuroscience Research Group, CEITEC – Central European Institute of Technology, Masaryk University, Brno, Czech Republic

[3]Multimodal and Functional Imaging Laboratory, CEITEC – Central European Institute of Technology, Masaryk University, Brno, Czech Republic

[4]Department of Economics, Faculty of Economics and Administration, Masaryk University, Brno, Czech Republic

[5]Department of Public Economics, Faculty of Economics and Administration, Masaryk University, Brno, Czech Republic

Correspondence
Daniel J. Shaw, Department of Psychology, Aston University, B4 7ET, UK.
Email: d.j.shaw@aston.ac.uk

Funding information
Grantová agentura České republiky (GA ČR), Grant/Award Number: GA16-18261S

Abstract

During social interactions, decision-making involves mutual reciprocity—each individual's choices are simultaneously a consequence of, and antecedent to those of their interaction partner. Neuroeconomic research has begun to unveil the brain networks underpinning social decision-making, but we know little about the patterns of neural connectivity within them that give rise to reciprocal choices. To investigate this, the present study measured the behaviour and brain function of pairs of individuals (N = 66) whilst they played multiple rounds of economic exchange comprising an iterated ultimatum game. During these exchanges, both players could attempt to maximise their overall monetary gain by reciprocating their opponent's prior behaviour—they could promote generosity by rewarding it, and/or discourage unfair play through retaliation. By adapting a model of reciprocity from experimental economics, we show that players' choices on each exchange are captured accurately by estimating their expected utility (EU) as a reciprocal reaction to their opponent's prior behaviour. We then demonstrate neural responses that map onto these reciprocal choices in two brain regions implicated in social decision-making: right anterior insula (AI) and anterior/anterior-mid cingulate cortex (aMCC). Finally, with behavioural Dynamic Causal Modelling, we identified player-specific patterns of effective connectivity between these brain regions with which we estimated each player's choices with over 70% accuracy; namely, bidirectional connections between AI and aMCC that are modulated differentially by estimates of EU from our reciprocity model. This input-state-output modelling procedure therefore reveals systematic brain–behaviour relationships associated with the reciprocal choices characterising interactive social decision-making.

KEYWORDS

anterior insula, anterior (mid-)cingulate cortex, behavioural Dynamic Causal Modelling, connectivity, iterated ultimatum game, reciprocity, social decision-making

1 | INTRODUCTION

Decision-making during repeated social interactions involves a dynamic process of mutual reciprocity, whereby the choices we make are simultaneously a cause and an effect of our interaction partners' behaviour. Over the course of a repeated dyadic exchange, for example, each interactant will reward or punish their partner's prior behaviour in an attempt to promote or discourage certain future behaviours. Neuroeconomic research has begun to elucidate the brain networks underpinning social decision-making during interactive contexts (Rilling & Sanfey, 2011), yet it remains unknown how patterns of neural connectivity within these networks give rise to reciprocal choices (e.g., Cáceda et al., 2017).

The ultimatum game (UG; Güth, Schmittberger, & Schwarze, 1982) presents an experimental paradigm with which to investigate

reciprocity during social interaction (see Krueger, Grafman, & McCabe, 2008). In this game, a Proposer is asked to divide a sum of money (the 'pie') between themselves and a Responder, who then chooses whether to accept or reject the proposed division. If the Responder accepts then the pie is divided accordingly, but if they reject, neither player receives any payoff. When played in a typical one-shot format, whereby the game ends after the Responder accepts or rejects a single proposal, modal offers are around 40% of the pie. This is believed to reflect strategic behaviour; to maximise their own payoff, Proposers refrain from offers that are likely to be rejected, such as those with which they earn disproportionately more (advantageous inequity). Indeed, Responders reject one-off proposals of 20% about half the time, suggesting they consider it unfair to be offered disproportionately less (disadvantageous inequity; Henrich et al., 2005). This standard format fails to capture the bidirectional property of repeated exchanges, however, in which reciprocal tendencies are likely to sway choices over multiple exchanges; Responders can retaliate against prior selfishness by temporarily lowering their tolerance for disadvantageous inequity, for instance, and Proposers can reciprocate with more equitable proposals. Alternatively, either player can adopt an unwavering strategy by offering or accepting only divisions that benefit themselves maximally. An iterated UG (iUG), then, allows for varying expressions of reciprocity to unfold during a simulated real-world dyadic interaction (Avrahami, Güth, Hertwig, Kareev, & Otsubo, 2013; van Damme et al., 2014).

A number of neuroimaging investigations have examined brain responses during the one-shot UG, and meta-analytic reviews reveal that Responders' rejections are associated reliably with neural responses in anterior insula (AI) and the dorsal anterior/anterior-mid cingulate cortices (aMCC; Feng, Luo, & Krueger, 2015; Gabay, Radua, Kempton, & Mehta, 2014). The aMCC is also implicated in Proposer behaviour, with strategic proposals eliciting electrocortical responses in frontal midline brain regions (Billeke et al., 2014; Billeke, Zamorano, Cosmelli, & Aboitiz, 2013; Wang, Li, Li, Wei, & Li, 2016). Given its diffuse connectivity profile, the AI is believed to integrate sensory, interoceptive and affective processes that together comprise emotional feeling states (Craig, 2009)—the same states likely to drive reciprocal choices. The aMCC appears to process and integrate social information necessary for predicting and monitoring the outcomes of decisions made during interactions, particularly those influencing the motivational state of our interaction partner(s) (Apps, Lockwood, & Balsters, 2013; Apps, Rushworth, & Chang, 2016). In this light, brain function within these two regions, and the degree of their functional connectedness, is likely to drive reciprocal behaviour.

Consistent with this notion, the strength of functional connectivity among a brain network comprising the AI and ACC has been shown to predict the tendency to reciprocate trust (Cáceda, James, Gutman, & Kilts, 2015). Furthermore, Feng et al. (2018) report that functional connectivity among a brain network encompassing the AI and ACC modulate egocentric biases expressed during fairness-related decisions, implicating this network in normative decision-making processes that might motivate the decision to reciprocate. Importantly, however, these studies did not investigate reciprocal behaviour, nor the underlying patterns of effective connectivity, during repeated exchanges between the same interactants. Bidirectional connectivity between these brain regions is proposed to permit the inference of others' feeling states that allow predictions of their future behaviour (Bernhardt & Singer, 2012; Medford & Critchley, 2010), and these inferences will develop over successive interactions with the same individual. As such, coordinated interactions between the AI and aMCC might guide reciprocal choices during an iUG between the same players.

The present study investigated this by performing functional magnetic resonance imaging (fMRI) on pairs of players whilst they interacted with one another on an iUG, and modelling player behaviour as reciprocal choices. The latter was achieved by adapting a model from experimental economics, fitting each player's round-by-round behaviour (the proposed division or its acceptance/rejection) to an estimate of expected utility (EU) on each exchange (Cox, Friedman, & Gjerstad, 2007). Crucially, this estimate considered not only the distribution of payoff between players, thereby incorporating any inequity aversion, but also the extent to which their choices reflect reciprocal reactions to their partner's prior behaviour; if player A considers B's past behaviour to have been fair then they will perceive greater utility in increasing B's relative payoff, but if A believes B's past behaviour to have been unfair they will see more utility in decreasing B's payoff (positive and negative reciprocity, respectively). Brain responses that map onto these round-by-round estimates of EU therefore reflect utility evaluations influenced by reciprocal tendencies. Given their consistent involvement in the UG reported by meta-analyses, their purported roles in social decision-making and their inclusion in brain networks implicated in reciprocity, we hypothesised that the AI and aMCC of both players would exhibit brain responses modulated by these estimates of EU. Furthermore, we predicted that patterns of AI–aMCC connectivity underlie reciprocal choices; specifically, that signals from AI in response to the prior behaviour of an interaction partner would serve as inputs to the aMCC, thereby modulating the response of the latter and, in turn, the resultant behavioural output (the choice of offer, or decision to accept/reject). This was achieved with behavioural Dynamic Causal Modelling (bDCM; Rigoux & Daunizeau, 2015), a technique capable of identifying patterns of directional (effective) connectivity within this two-node network, how this connectivity profile is influenced by EU and if it can be used to estimate choices on the iUG.

2 | METHODS

2.1 | Participants

The initial sample comprised 70 males recruited from Masaryk University, Czech Republic, who were paired to form 35 Proposer–Responder dyads. The individuals comprising each dyad had never met prior to the day of the experiment. Male–male dyads were measured exclusively to avoid any potentially confounding factors associated with mixed-sex interactions. Poor behavioural or neuroimaging data from one Proposer and one Responder comprising two different dyads led to the omission of two pairs (see below). The 66 males forming the remaining 33 dyads had a mean age of 30.6 years (*SD* = 11.0; range = 19–65; mean intra-dyad age difference = 2.1 years); all reported normal or corrected-to-normal vision

and no history of neurological diseases or psychiatric diagnosis. All participants provided informed consent prior to the experimental procedure, which was approved by the Research Ethics Committee of Masaryk University.

2.2 | Procedure

On the day of the experiment, the Proposer and Responder of a given pair met for first time and exchanged names before being sent to one of two scanners located in adjacent rooms. Player roles were assigned randomly at the start of scanning but remained fixed throughout the experiment, one participant playing the role of Proposer and the other playing Responder on all rounds. Fixing the roles in this way allowed players to learn about and adapt to (reciprocate) their partner's behaviour over a relatively short period. Prior to the experiment, players were told explicitly that throughout the scanning procedure they would play with the same individual to whom they had just been introduced, and that their respective roles would remain fixed. Functional scanning was conducted in a single session, comprising 60 rounds (events) of the iUG and 30 rounds of a control condition (CTRL; see below) performed in an event-related fashion. Each UG round began with the Proposer being given 4 s to choose between two divisions of the pie (the 'choice set'; see below) between themselves and the Responder (*Choice*). Only after this 4 s period was the Proposer's offer highlighted for a further 4 s (*Offer*), during which the Responder chose to accept or reject the proposal. Again, only after this period was the Responder's decision presented for a final 4 s (*Decision*). The same procedure was followed on CTRL rounds, but the choice set comprised two alternative divisions of colour. An example UG and CTRL round is illustrated in Figure 1. Importantly, the stimuli comprising each round were presented simultaneously to both players who observed the exact same stimulus sequence—Responders saw the choice set from which Proposers selected their offer, and Proposers saw the Responder's decision to accept/reject the proposal. Players gave their choices via two-button response boxes. All rounds ended with a jittered inter-trial interval, with a fixation cross presented for 2–4 s (mean = 3). The same pseudo-randomised intermixed sequence of UG and CTRL choice sets was used for all pairs, which was defined by a genetic algorithm for design optimisation set to maximise contrast detection between conditions (Wager & Nichols, 2003). Participants received the monetary outcome of six UG rounds selected randomly [mean reward = 240 CZK (approx. €9)]. Players were never informed about the choice sets they would encounter, nor the number of remaining rounds during the experiment (see Supporting Information for participant instructions).

As part of a separate ongoing study, after the iUG each player completed two self-reports instruments measuring components of personality—the Action Control Scale (ACS-90; (Kuhl, 1994) and Interpersonal Reactivity Index (Davis, 1983). As an exploratory analysis, we assessed whether performance on the iUG and metrics of effective connectivity estimated by bDCM were related to personality variables measured by these instruments. Given the exploratory, post hoc nature of these analyses, however, we do not present the results here. Instead, the reader can consult them in Table S4, Supporting Information.

2.3 | UG stimuli

Each of the 60 UG rounds presented players with a choice set consisting of two divisions of 100 Kč (approx. €4), from which Proposers were required to select one as their offer to the Responder. From the Proposers' perspective, the two divisions differed in magnitude of advantageous inequity; on 30 rounds they had to choose between

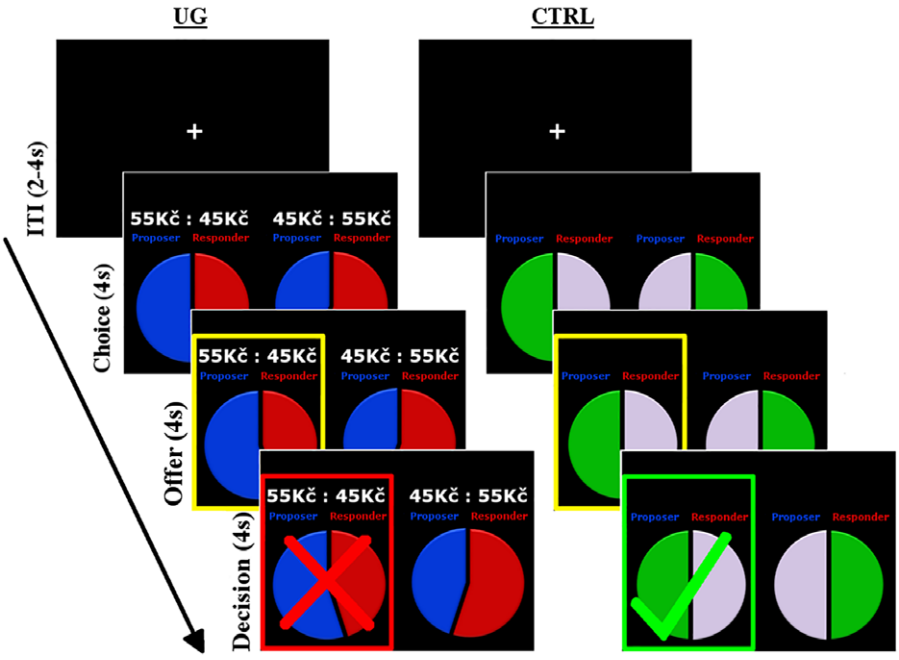

FIGURE 1 Example UG (left) and CTRL round (right), comprising 4-s Choice, Offer and Decision periods. In these examples, the offer made by the Proposer on the UG round is rejected by the Responder, whilst the offer made on the CTRL round is accepted [Color figure can be viewed at wileyonlinelibrary.com]

maximal and minimal advantageous inequity (e.g., 70:30|60:40), and for the other 30 UG rounds, they were required to choose between advantageous and disadvantageous inequity (e.g., 60:40|40:60). For the sake of brevity, herein we refer to the former division of each type of choice set as the selfish division, and the latter as the generous division. Together, these two types of choice sets were intended to maximise expressions of reciprocity between players: For those in which the Proposer incurred a greater relative cost by being generous, they were more justified in offering the selfish division and, in turn, expressed greater co-operative intent when offering the generous division. Conversely, when the relative cost to the Proposer was minimised in offering the generous division, a selfish offer (SO) indicated less co-operative, more egoistic motives. To optimise our modelling procedures applied to behavioural and brain data, all UG rounds were combined. Table S1 lists the 10 choice sets used in the experiment, which were pseudo-randomised and intermixed among CTRL rounds (see above). Importantly, pseudo-randomisation ensured an even distribution of each choice set throughout the procedure, such that no choice was presented twice in succession. One Responder chose to accept all proposals, regardless of their payout. Data from this individual and their corresponding Proposer were excluded from all analyses.

2.4 | Imaging protocol

As part of a dual-fMRI protocol, functional and structural MR data were acquired from each player comprising a dyad simultaneously with one of two identical 3T Siemens Prisma scanners equipped with a 64-channel bird-cage head coil. Players were allocated to one of the two scanners in a counterbalanced fashion, ensuring an even number of Proposers and Responders were scanned in each. Blood-oxygen-level-dependent (BOLD) images were acquired with a T_2*-weighted echo-planar imaging (EPI) sequence with parallel acquisition (i-PAT; GRAPPA acceleration factor = 2; 34 axial slices; TR/TE = 2000/35 ms; flip angle = 60°; matrix = 68 × 68 × 34, 3 × 3 × 4 mm^3 voxels). Axial slices were acquired in interleaved order, each oriented parallel to a line connecting the base of the cerebellum to the base of orbitofrontal cortex; this permitted whole-brain coverage. Functional imaging was performed in a single run comprising 690 volumes (23 min), with four dummy volumes acquired at the beginning to allow the gradients to reach steady state. A high-resolution T_1-weighted structural MR image was acquired prior to the functional run for localisation and co-registration of the functional time series (MPRAGE, TR/TE = 2,300/2.34 md; flip angle = 8°; matrix = 240 × 224 × 224, 1 mm^3 voxels).

2.5 | Preprocessing

Neuroimaging data were preprocessed with SPM12 (http://www.fil.ion.ucl.ac.uk/spm), which involved spatial realignment and unwarping, slice-time correction, normalisation and spatial smoothing. Motion correction was performed using a six-parameter rigid-body transformation, with the first functional scan as a reference. Six motion parameters estimated from this realignment processed were used subsequently as nuisance covariates to account for motion-related variance. One Proposer exceeded our exclusion criterion of 2 mm of movement in any direction between successive volumes; data from this participant and their opponent were omitted from all subsequent analyses. Initial attempts to normalise the functional time series to the Montreal Neurologic Institute (MNI) T1 template failed for several subjects, so we used non-linear transformations (trilinear interpolation; 16 warping iterations) to co-register the mean of the motion-corrected fMRI volumes to the EPI template in MNI space. To maximise the quality of this normalisation process, we used the *mask_explorer* tool (Gajdoš, Mikl, & Mareček, 2016). Images were then smoothed with a 5-mm isotropic Gaussian kernel, and a high-pass filter with 128 s cut-off removed low-frequency drifts.

2.6 | Reciprocity model

Cox et al.'s (2007) model of reciprocity extends other distributional preference models that consider only the final relative payoff between players (Bolton & Ockenfels, 2000; Fehr & Schmidt, 1999); specifically, it attempts to fit the behavioural observation that choices depend not only on the final distribution of payoff, but also on any available alternatives. More importantly, it also considers players' choices to be influenced by reciprocal tendencies. Unlike higher belief equilibrium models (Charness & Rabin, 2002; Falk & Fischbacher, 2006), the reciprocity model is tractable and enables the estimation of behavioural parameters; it provides an estimate of the degree to which a player's proposals, or their decisions to accept/reject an offer reflects reciprocal reactions to their opponent's prior behaviour.

In our adaptation, for each player, the EU of a division of the pie was specified as:

$$U(x,100-x) = x + (\theta+\epsilon)(100-x) \quad (1)$$

In Equation (1), x is the player's portion of a division, θ is a scalar that represents their emotional state and ϵ is a random variable with standard logistic distribution representing an unobserved component of the utility function—an error term that adds stochasticity to the player's choice behaviour (e.g., unintended responses). The emotional state was formulated as:

$$\theta = \alpha_i(x-x_0) \quad (2)$$

Equation (2) incorporates a player-specific reciprocity parameter, α, which weighs a comparison of the player's share, x, against a fairness reference point, x_0, by the extent to which the player's choices are influenced by their opponent's prior behaviour. Whilst α_i is the time invariant, the reference point, x_0, is different for each choice set and therefore changes on each round. In other words, $\theta > 0$ on a given round represents a player's affective response to their opponent's prior behaviour, driven by their evaluation of fairness at that point in the game and their overall tendency to reciprocate across the iUG.

We modelled round-by-round EU for both players based upon this utility function; the Responder accepts a proposal if:

$$x + (\theta+\epsilon)(100-x) > 0 \quad (3)$$

The Proposer offers the generous division if:

$$P_1(x_1 + (\theta+\epsilon)(100-x_1)) > P_2(x_2 + (\theta+\epsilon)(100-x_2)) \quad (4)$$

From the Proposer's perspective, x_1 and x_2 in Equation (4) represent the generous and selfish division, respectively and P_i represents

the probability that the Responder will accept a division given their prior behaviour. In other words, the Proposer makes a SO that benefits themselves maximally only if they believe the offer is likely to be accepted. To capture the expectation of acceptance on a given round, our model estimated the range of preceding rounds that maximised the log-likelihood of the Proposer model (predicted Proposers' offers with highest accuracy). This is referred to as the *memory* [*M*] parameter, which was estimated at the group level from the decisions of all Responders. Importantly, *M* was estimated only for Proposers because their payoff on a given round depends upon the expected (unknown) decision of the Responder; conversely, the round-by-round payoff for the Responder depends upon the Proposer's offer, which is known. The Supporting Information details the procedures through which the various parameters were estimated.

2.6.1 | General linear modelling

General linear modelling (GLM) was performed on the preprocessed time series in a two-step process using SPM12 (http://www.fil.ion.ucl.ac.uk). First, within-subject fixed-effect analyses were used for parameter estimation at the individual level. Event-related responses were modelled as the period of rounds in which a player made their choices, with durations determined by their response time: To capture brain responses that reflected each player's reciprocal reactions to their partner's prior behaviour, for Proposers, we modelled the *Choice* period of each round until an offer was selected, whilst for Responders it covered the *Offer* period until a decision had been made to accept or reject the proposed division (see *Behaviour*). Using response times in this way served to introduce further jitter, optimising the estimation of brain responses underlying choices. The remaining parts of the rounds were modelled as regressors of no interest. These responses were then convolved with a canonical hemodynamic response function. For UG rounds, we added parametric modulators that expressed the round-by-round EU estimated with the reciprocity model (UG_{MOD}). Statistical evaluations of the first-level parameter estimates were performed with group-level whole-brain random-effects contrasts, with cluster-level family wise error (FWE) correction for multiple comparisons across space. Given the wide age range of our sample, and the observation that participant age contributes to the degree of variability in expressions of reciprocity (Cáceda et al., 2015), we compared these group-level estimates of EU-modulated brain responses to the same model with age entered as an additional group-level covariate.

2.6.2 | Behavioural DCM

DCM is a mathematical technique that models how information enters, propagates and reverberates throughout a brain network (Friston, Harrison, & Penny, 2003). In an extension of this, bDCM attempts to fit such stimulus-induced changes in effective connectivity to behavioural outcomes—it performs a neurocognitive decomposition of the input-state-output transfer function. A detailed description of the estimation process behind bDCM is provided in Rigoux and Daunizeau (2015), and a description of this process as applied to our data is given in the Supporting Information. Below, we summarise the primary components.

In our implementation, bDCM estimated three sets of parameters: (*A*) A pattern of task-independent endogenous connectivity between the AI and aMCC, representing the directional influence(s) between these two nodes at rest (see below); (*B*) task-dependent modulation of these endogenous connections, representing their round-by-round perturbation by estimates of EU from our reciprocity model and (*C*) the direct influence of an experimental stimulus (presentation of the choice set for Proposers, and the offer for Responders) on a network node, modelled as an unconvolved regressor representing the *Choice* (Proposer) or *Offer* (Responder) period before the player made their choice. Through a combined influence of these three parameters, bDCM then estimated a player's choices (*hA*). It is important to note that, in order to optimise the modelling procedure, the behaviour of each player was expressed as a binary function—that is, whether a generous (1) or selfish division (0) was offered by the Proposer, and if the offer was accepted (1) or rejected (0) by the Responder.

Parameter estimation was performed with the Variational Bayesian Analysis toolbox of MATLAB (Daunizeau, Adam, & Rigoux, 2014). In a hypothesis-driven approach, the *A* parameter was set according to the meta-analytic results of Feng et al. (2015); namely, volumes of interest (VOIs; spheres of 10 mm radius) were centred on coordinates within the right AI (x = 38, y = 20, z = 0) and aMCC (x = 8, y = 22, z = 40) that expressed the contrast fair > unfair offers maximally across 11 neuroimaging studies employing the UG. From these VOIs, we extracted the first eigenvariate of all time series from voxels expressing the UG > CTRL contrast in the GLM analysis (p_{FWE} < .001). Structural (endogenous) models of causal connectivity between the VOIs modelled the hypothesised brain state. All neurophysiologically feasible models were evaluated with Variational Bayes (VB) inversion, which rated the likelihood of each with log model evidences. Fourteen models were evaluated, defined by logical combinations of the *A*, *B*, *C* and *hA* parameters. As shown in Figure 2, the model space comprised those with both uni- and bi-directional intrinsic connections between the two regions (*A* parameter), the modulatory influence of EU on either the nodes themselves or their interconnections (*B* parameter), and direct stimulus input to either node (*C* parameter). Logical combinations of intrinsic nodal connectivity and direct nodal input restricted the number of model comparisons; for example, a model with direct input to AI and a unidirectional endogenous connection from aMCC to AI would not permit input–output information flow through the circuit, and was therefore not considered. Furthermore, given its purported role in translating cognitive processes into action, only models where the behavioural response is driven by aMCC were considered. After VB inversion, we assessed the log model evidences for all models and subjects using a random-effect Bayesian model selection (RFX BMS) procedure.

This produced approximated exceedance probabilities (AEPs) and estimated model frequencies (EMFs), goodness-of-fit indices based upon the free energy of all compared models that reflect how well a given model fits both the BOLD and behavioural time series (the latter representing the binarised choices of each player in each round). The AEP identifies the relative superiority of one model compared to all others comprising the model space (Penny, Stephan, Mechelli, & Friston, 2004; Stephan et al., 2007), and the model earning the highest exceedance probability is defined as the optimal model; a value of 0.8

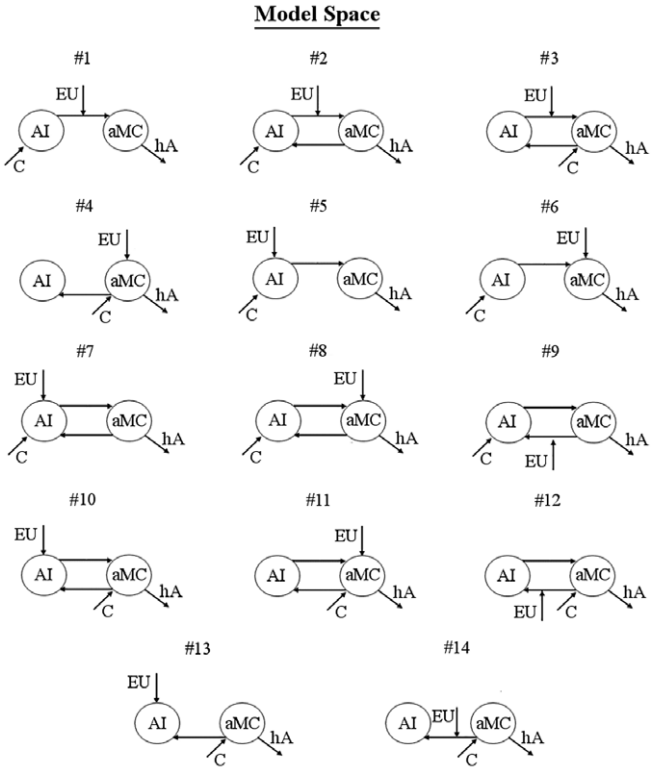

FIGURE 2 Models evaluated with Bayesian model selection. Models comprise either a single unidirectional or bidirectional intrinsic connections from right anterior insula (AI) to right anterior/anterior-mid cingulate cortex (aMCC), but vary in the target of EU modulation

indicates that the model is 80% more likely to be better than other model given the data. The EMF provides an estimate of the prevalence of each tested model in the population (Rigoux, Stephan, Friston, & Daunizeau, 2014; Stephan et al., 2009). Importantly, it is not possible to infer whether the neuroimaging or behavioural data drives the fit indicated by the AEP or EMF. For this reason, we also computed a behavioural fit precision (BFP) index, which is computed directly from a comparison of the measured and modelled behavioural responses—for each subject, it represents the amount of matches between their real/observed and estimated time series divided by the total number of responses.

3 | RESULTS

3.1 | Behaviour

To assess whether player choices were driven solely by monetary payoff, we first examined performance across the 10 different choice sets used on UG rounds (see Figure 3a). As shown in Table 1, Spearman correlations revealed that neither players' RTs were related significantly to their payoff in the selfish division. To assess whether RTs were influenced more by the degree of inequity presented by the choice set, we calculated the difference between the log ratios of the two divisions comprising each choice set; higher values of this

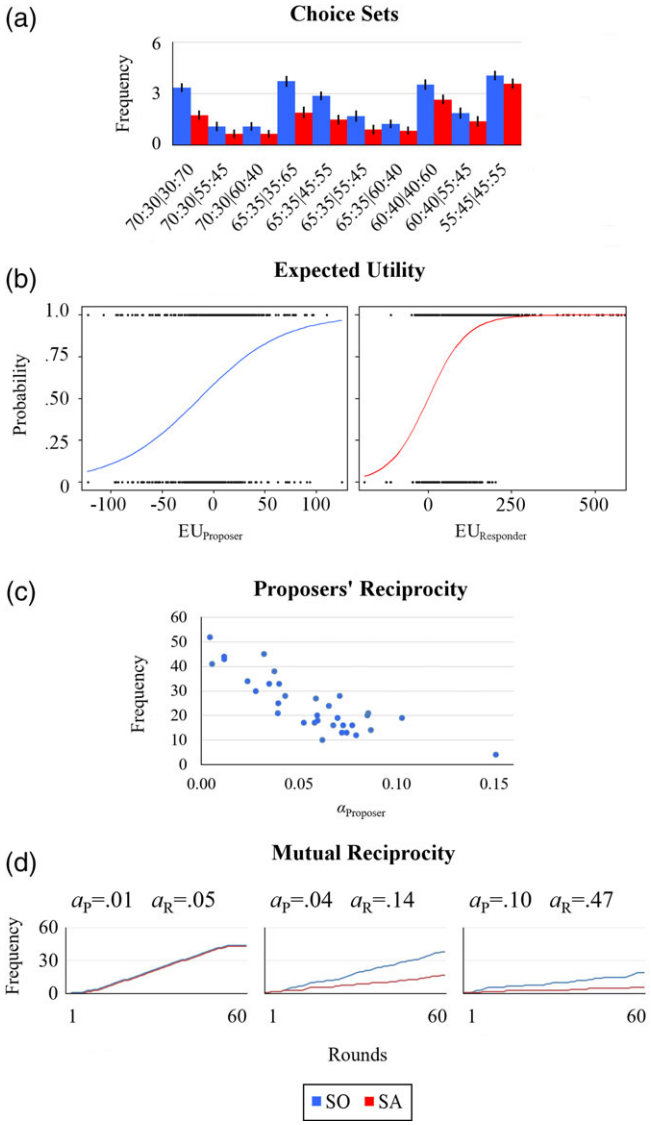

FIGURE 3 Player behaviour. (a) Mean frequency of selfish offers (SO) and their acceptance (SA) for each of the 10 choice sets. Error bars present *SE*. (b) Probabilities of SO and SA plotted as a logistic function of expected utility (EU), as estimated with the reciprocity model. (c) The proportion of SO plotted as a function of Proposers' reciprocity (α), as estimated by the reciprocity model. This reveals that with increasing reciprocity, Proposers were less likely to offer the division that benefited themselves maximally. (d) Cumulative frequencies of SOs and SAs over all 60 UG rounds, for three example dyads. For the leftmost dyad, estimates of reciprocity were low for both the Proposer (α_P) and Responder (α_R). This is reflected in high number of SOs and SAs; the Proposer was free to offer selfish divisions because the Responder did not challenge such proposals with rejections (negative reciprocity). In the middle dyad, the Responder did challenge SOs and this is reflected in a higher reciprocity estimate. These rejections did not alter the Proposer's behaviour, however; they continued to propose SOs, reflected in a low reciprocity estimate. In the rightmost dyad, estimates of reciprocity were high for both the Proposer and Responder, and this is reflected in a low number of SOs and SAs; the Responder was unwilling to accept selfish divisions, and the Proposer responded with fewer selfish proposals [Color figure can be viewed at wileyonlinelibrary.com]

TABLE 1 Correlations among indices of performance over the iUG and the 10 different choice sets, for Proposers (top) and Responders (bottom)

		Payoff SO	Inequity	SO/SA	RT
Proposer	Payoff SO	1			
		–			
	Inequity	.46	1		
		[−.20,.85]	–		
	SO	−.62	.32	1	
		[−.97,.01]	[−.39,.79]	–	1
	RT	−.33	.47	.82**	–
		[−.88,.46]	[−.29,.89]	[.37,.97]	
Responders	Payoff SO	1			
		–			
	Inequity	−.46	1		
		[−.87,.22]	–		
	SA	.66*	.29	1	
		[−.02,.99]	[−.38,.77]	–	
	RT	.40	.44	.71*	1
		[−.34,.87]	[−.32,.77]	[.01,.99]	–

RT = response time; SA = selfish offer acceptance; SO = selfish offer/division. *Note.* Values in square brackets present the confidence intervals computed from 1,000 bootstraped samples. *$p < .05$. **$p < .01$ (two-tailed).

inequity coefficient represented a greater difference in inequity between the constituent divisions (e.g., 70:30|30:70 vs. 55:45|45:55; see Table S1, Supporting Information). Neither Proposers' nor Responders' RTs were correlated significantly with this coefficient. It is important to acknowledge that the lack of relationship between Responder RTs in the Offer period and other measures of UG performance might reflect the simultaneous presentation of stimuli to both players; Responders may have begun to evaluate the constituent divisions during the Choice period, making their RTs in the Offer period less representative of their decision-making process. Indeed, Responders' RTs were significantly shorter than those of Proposers [1,268.10 ($SD \pm 491.34$) vs. 2,165.64 ($\pm$409.95) m; $t_{[64]} = 8.06$, $p < .001$, $d = 1.98$].

We then examined patterns of choices over the different choice sets and proposed divisions; namely, the number of rounds on which the selfish of the two divisions was offered (SO), and the number of these offers that were accepted [selfish-offer acceptance (SA)]. In Proposers, the number of SOs for given choice set was not correlated with their relative payoff for the selfish division, but the number of SAs by Responders was correlated positively with their own payoff. The number of SOs and SAs was unrelated to the inequity coefficient. Together, these results indicate that Proposers' choices were influenced by factors other than their own monetary payoff (or cost) or the distribution of payoff between players. Responders showed some influence of payoff, but the strength of this association would be stronger should their choices be driven purely by monetary gain. This might explain why neither players' RTs tracked with the absolute or relative payoff.

Next, we applied our adapted reciprocity model to the behavioural data of each player measured throughout the iUG to estimate the degree to which each individual's choices reflected reactions to their interaction partner's prior behaviour. For Proposers, greater values of EU represent higher utility for the more generous division within a choice set; whilst for Responders, it represented greater utility in accepting a proposed division. As shown in Figure 3b, the probability of SOs and SAs varied according to the estimates of EU from our reciprocity model; the model correctly estimated the choices of Proposers and Responders on 70.05 [$\pm$0.01 (Log-likelihood = −1,070.6; Akaike Information Criterion (AIC) = 2,207.2)] and 81.81 ($\pm$0.01) % of UG rounds (Log-likelihood = −677.8; AIC = 1,421.6), respectively. The model produced a reciprocity parameter, α, for each Proposer and Responder, which were lower for the former (.06 [.01]) compared with the latter (.12 [$\pm$.02]) than; $t_{[38.3]} = 9.61$, $p < .001$); Proposers' decisions reflected stronger reactions to their partner's decisions. Interestingly, however, α estimates for Proposers were correlated negatively with the number of SOs they proposed ($r_{[32]} = -.84$ [.73, .90] $p < .001$); the more reciprocity they exhibited, the less likely they were to propose divisions that benefited themselves maximally (see Figure 3c). No such relationship was observed between Responders' α and SAs ($\rho_{[17]} = -.01$ [−.32, .37], $p = .942$). Across all Proposers, the optimal *M* parameter was 56. Whilst this identified the range of preceding rounds that maximised the accuracy of estimates for Proposers' offers, accuracy increased only subtly beyond a range of 20 (see Table S3).

To evaluate our reciprocity model more formally, we compared it against a variety of alternative models (see Supporting Information for details on model specifications). First, we tested a nested model by fixing the reciprocity parameter to $\alpha = 0$ for both players—a self-regarding model that evaluated the reciprocity parameter by testing the assumption that both players care only about their own monetary payoff. A likelihood ratio test (*L*) and AIC comparison demonstrated that our reciprocity model outperformed this simple monetary model for both Proposers (AIC = 2,925.1; $L_{[33]} = 811.00$, $p < .001$) and Responders (AIC = 1900.5; $L_{[33]} = 544.90$, $p < .001$). We then assessed whether player choices reflect learning processes over multiple rounds rather than reciprocal reactions by modelling each player's behavioural data with a three-parameter reinforcement learning

model (Erev & Roth, 1998). This model contains a forgetting parameter φ, an experimentation parameter ε, and a strength parameter *s* (an extension of the simple one-parameter reinforcement learning model, in which φ = 1 and ε = 0). Each parameter was fitted to maximise the log-likelihood function, separately for Proposers (φ = 0.91, ε = 0.15, *s* = 5.6) and Responders (φ = 0.84, ε = 0.15, *s* = 6.00). Again, an AIC comparison revealed that the fit of our reciprocity model significantly outperformed this reinforcement learning model for both Proposers (AIC = 2,492) and Responders (AIC = 1,794).

Finally, from a game theoretic perspective, our reciprocity model might be considered inappropriate for the repeated nature of our iUG; players might have planned their moves at the beginning of the game, taking into account that at every stage (round) their action (choice) will have an immediate payoff and also affect the continuation value in the rest of the game (Mailath & Samuelson, 2006). To assess this, we also evaluated our reciprocity model against one that modelled each player's choices in terms of a fixed strategy over all rounds. Since the set of possible strategies is infinite, some a priori restriction on the set of strategies was needed. We evaluated 12 reasonable strategies that players might have followed (see Table S2). For each player, we then took the strategy that matched their actual choices on most rounds (the strategy with the highest likelihood) and calculated the fit of the overall model. A comparison revealed that this alternative model estimated both player's decisions with less accuracy than our reciprocity model: For Responders, the log-likelihood was −792.2 (AIC: −1,586.4) and their choices deviated from the maximally fitting strategy on 15% of rounds. Similarly, the log-likelihood of the Proposer model was −1,128.17 (AIC: −2,282.3), and their choices deviated from their best-fitting strategy on 32% of rounds.

3.2 | General linear modelling

Whole-brain GLM revealed diffuse clusters of BOLD signal expressing the UG_{MOD} > CTRL contrast in both Proposers and Responders; that is, brain responses modulated parametrically by EU estimated with our reciprocity model. No significant differences were observed between player roles for this contrast, and Table 2 presents the peak co-ordinates of all clusters for both players separately to illustrate their similarity. These clusters encompassed lateral and medial prefrontal, posterior parietal and inferior occipital cortices, thalamic nuclei and the ventral striatum (e.g., caudate nucleus). As shown in Figure 4a, the GLM analysis revealed strong EU modulation in the meta-analytic-defined co-ordinates of the right AI and aMCC from which BOLD signal was extracted for the bDCM analysis. No significant differences were observed between these brain responses modulated by EU and those modulated additionally by age, even a very lenient uncorrected level ($p < .05$). This indicates no additional influence of age on EU-modulated BOLD signal.

3.3 | Behavioural DCM

The optimal patterns of effective connectivity between the meta-analytically defined AI and aMCC, as identified by RFX BMS, are presented in Figure 5a.

As shown in Table 3, for Proposers, both the AEP and EMF parameters converged to reveal Model 9 as the optimal model, the free energy of which exceeded that of the confidence intervals for the null hypothesis (see Figure 5b). The BFP index revealed that, across all Proposers, an average of 71.45 (±9.22) % of choices matched those estimated from the bDCM procedure—namely, whether they decided to propose the more generous of the two divisions. This model comprises bidirectional connections between AI to aMCC, with round-by-round estimates of EU modulating the aMCC-to-AI feedback connection. Through this circuit, presentation of the choice set elicits increased BOLD response within the AI (.02 Hz), which then sends excitatory signals to aMCC (.52 Hz). The aMCC then sends inhibitory feedback to AI (−.38 Hz), the strength of which is modulated negatively by EU (−.05 Hz); as such, the inhibitory feedback becomes weaker (less negative) with greater EU for the more generous division. As a result of the elevated BOLD response in aMCC, generous offers are more likely (.11 Hz)—in other words, as a result of signal conduction through this circuit, with greater EU for the generous division, the Proposer is more likely to make a generous offer.

For Responders, both AEP and EMF parameters revealed that Model 2 was the winning model, and the free energy of this model exceeded the confidence intervals for the null hypothesis (see Figure 5b). The BFP indicated that, across all Responders, through this model the bDCM procedure correctly estimated the decision to accept a proposal on 84.25 (±11.01) % of UG rounds. This model again comprises bidirectional connections between AI and aMCC. Presentation of the offer elevates the BOLD response of AI (.06 Hz), which sends excitatory signals to aMCC (.50 Hz). Then, through the aMCC-to-AI connection, the aMCC sends inhibitory feedback signals to AI (−.39 Hz). The elevated BOLD response in aMCC serves to increase the likelihood of acceptance (.04 Hz), and the feedforward AI-to-aMCC connection is modulated positively by round-by-round estimates of EU (.01 Hz). In other words, with greater EU for the proposed division, there is an increased likelihood of acceptance.

4 | DISCUSSION

This study investigated the brain processes underlying the bidirectional reciprocity characterising social decision-making. To this end, we investigated if the choices made by two interacting individuals over recursive economic exchanges could be estimated by specific patterns of connectivity between the right AI and aMCC. Players' decisions on each round were modelled as EU in a way that captured their expression of reciprocity—that is, the extent to which their choices on each exchange reflect reactions to their opponent's prior choices. Estimates of EU modulated the brain response of both regions and patterns of effective connectivity between them, and this, in turn, estimated player choices with high accuracy.

It is important to restate that, from a game theoretic perspective, our reciprocity model might seem inappropriate for the repeated nature of our iUG design. Since the choice set changed on each round, however, our iUG did not involve a repetition of the same stage game. Furthermore, the strategies employed during a repeated interaction are likely to be highly complex, making it impossible to distinguish

TABLE 2 Brain regions exhibiting EU-modulated responses

		Proposer					Responder				
Label		**Voxels**	**Peak**	***x***	***y***	***z***	**Voxels**	**Peak**	***x***	***y***	***z***
Frontal pole	R						305	9.54	33	53	25
MFG	L						36	6.66	−27	32	25
	R	73	7.43	33	−1	64					
IFG	R	30	7.15	51	5	28					
Insula/IFG*	R	177	10.78	54	17	−8					
Insula	L	424	8.47	−39	−1	4	444	9.36	−42	−4	13
	R						296	10.52	42	−4	10
Pallidum	R	22	6.36	15	8	−2					
Thalamus	L	81	7.35	−12	−28	7					
	R						68	7.38	12	−19	4
Precentral gyrus	L	496	8.70	−3	−13	76					
Postcentral gyrus	L						828	10.45	−60	−25	40
	R	764	10.57	42	−37	61					
IPS	L	892	10.06	−54	−25	49					
LOC	L						633	9.87	−39	−82	−11
	R						1876	10.18	27	−61	37
IOG/Fusiform gyrus	L						25	5.51	−27	−91	13
	R	892	9.13	30	−82	−14	202	7.61	12	−103	4
Cerebellum	L	1,135	11.65	−36	−55	−32					
	R	41	6.75	18	−70	−47	29	6.18	48	−58	−29

MFG = middle frontal gyrus; IFG = inferior frontal gyrus; IPS = intraparietal sulcus; LOC = lateral occipital cortex; IOG = inferior occipital gyrus; PCC = posterior cingulate cortex. The table lists clusters of voxels expressing the UG_{MOD} > CTRL contrast (p_{FEW} < .001, k > 20 voxels), for both Proposers (left) and Responders (right). Coordinates are specified in MNI space, and voxels are given at 3 mm^3 resolution. *Clusters extend into VOIs used for behavioural Dynamic Causal Modelling analyses.

utility function parameters from them: Consider a player with a high value for their reciprocity parameter—this player has a strong tendency to punish unfair play or reward fair behaviour, but such a behavioural pattern is indistinguishable from a tit-for-tat strategy. As such, any attempt to model the behaviour as a repeated game would require additional assumptions about possible strategies to escape the folk theorem. By considering only players' expressions of reciprocity, our model has reduced the complexity of strategies whilst still estimating choices with high accuracy. This provides a new model for future research.

Reciprocity emerges as an indirect chain of inter-brain processes; through neural coupling, one individual's brain activity results in a behavioural output, which then elicits systematic neural responses in their interaction partner to initiate a behavioural reaction (Hasson & Frith, 2016). We have shown that the choices of two individuals engaged in economic exchanges fit closely with estimates of EU that reflect their round-by-round reactions towards their interaction partner. Whilst this deviates from game-theoretic assumptions that players choose a strategy at the beginning of the game and stick with it throughout, it fits with other observations of choice behaviour; Johnson, Camerer, and Rymon (2002), for instance, demonstrated that individuals engaged in a multiple-round bargaining experiment focus on the current round when making choices rather than planning their behaviour in advance. Brain responses that map onto these round-by-round estimates of EU in each player therefore exhibit such neural coupling. Given their consistent involvement in the UG (Feng et al., 2015; Gabay et al., 2014), and in social decision-making more generally (Rilling & Sanfey, 2011), it is perhaps unsurprising to see such neural coupling within the AI and aMCC. What is surprising, however, is that the reciprocal choices of both players can be estimated accurately by modelling patterns of effective connectivity between just these two brain regions. Within this simple network, the Proposer's decision to reward themselves or their interaction partner maximally, and the Responder's decision to accept or reject a division, involves the propagation of excitatory neural signals from the AI to the aMCC. The aMCC then determines the player's choice, whilst also sending inhibitory feedback signals to the AI. In Proposers, greater utility of the more generous division served to downregulate the feedback connection; with greater EU they were more likely to make a generous offer, and this connection became less inhibitory. Since the AI is involved in affective feeling states, an attenuation of the feedback connection with more generous offers (which incurs a greater relative cost to the Proposer) might therefore reflect a greater emotional reaction *caused by* the choice. In contrast, the positive modulation of the feedforward connection from AI to aMCC in Responders during offers with greater EU, which were more likely to be accepted, might reflect a positive affective response that provides a motivational *cause* for acceptance. Future studies should utilise other corollary measures of affectivity (e.g., skin conductance) to assess if and how emotional states influence reciprocal choices on the iUG.

Tract-tracing studies in non-human primates have demonstrated that the insula cortex is connected densely and reciprocally with not only the anatomically defined anterior cingulate cortex (ACC), but all association cortices, orbitofrontal and dorsolateral prefrontal cortices,

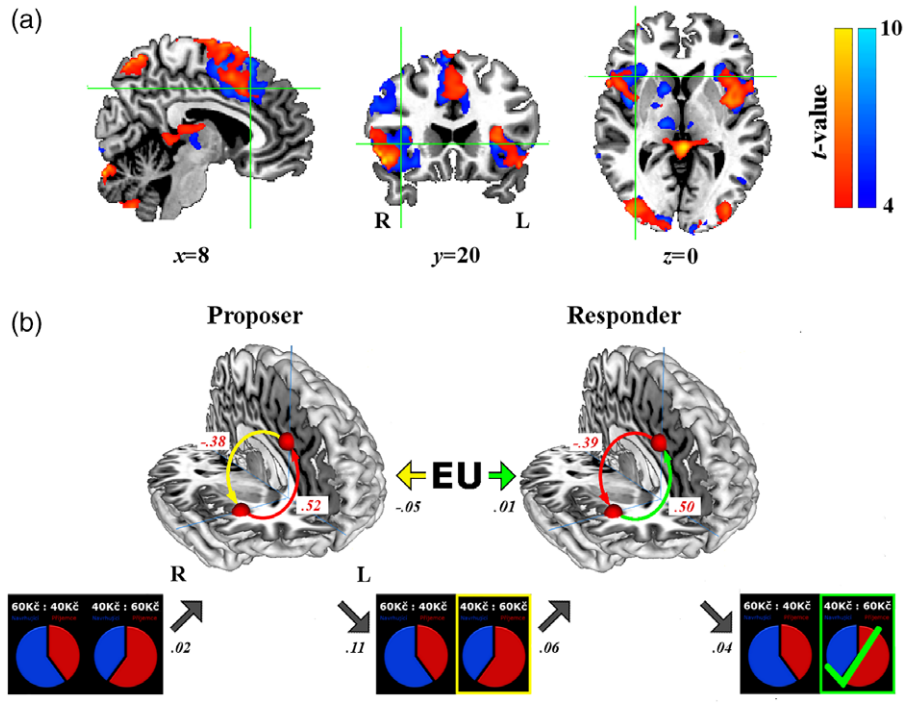

FIGURE 4 Neuroimaging results. (a) Thresholded parametric maps for the UG_{MOD} > CTRL contrast evaluated with general linear modelling, showing brain responses modulated by expected utility (EU) in Proposers (blue) and Responders (orange). Crosshairs show the coordinates used as the centre of gravity for the anterior-mid cingulate cortex (sagittal slice; $x = 8$, $y = 22$, $z = 40$) and right AI volumes of interest (coronal and axial slices; $x = 38$, $y = 20$, $z = 0$) from which BOLD signal was extracted for behavioural Dynamic Causal Modelling (bDCM). These coordinates were defined by the meta-analytic results of Feng et al. (2015). (b) Results of the bDCM analyses. Estimates of EU from the reciprocity model modulated the inhibitory feedback connection in Proposers (yellow arrow); and the excitatory feedforward connection in Responders (green arrow). Note: Parameters values represent the degree of influence on the brain circuit or behaviour (black arrows) or the strength of effective connectivity (red arrows), expressed in hertz

temporolimbic structures (e.g., amygdala), the thalamus, basal ganglia and brain stem nuclei (Augustine, 1996; Mesulam & Mufson, 1982a, 1982b). Neuroimaging of the human brain demonstrates an anterior–posterior distinction within the insula, whilst the anterior extent is connected structurally with ACC, frontal, orbitofrontal and anterior temporal areas, the posterior aspect possesses structural connections with parietal and sensorimotor cortices (for a review, see Uddin, 2015). This fits with the functional anatomy of the insula cortex; meta-analyses converge to delineate between the socio-emotional and cognitive functions of the ventral and dorsal anterior aspect, respectively, and the sensorimotor profile of the posterior insula (Kelly et al., 2012; Kurth, Zilles, Fox, Laird, & Eickhoff, 2010). Such connectivity places AI in an ideal position to integrate the sensory, cognitive and affective signals necessary for subjective feeling states (Craig, 2009). In this way, the AI is capable of exerting strong influences on cognition; by associating stimuli with internal feeling states it determines their relative salience and the cognitive resources allocated for their processing. By extension, the AI has the capacity to influence motivational processes; by associating stimuli with positive or negative feeling states it encodes their incentive value, motivating approach or avoidance behaviour (Namkung, Kim, & Sawa, 2017). Our observation of EU-modulated brain responses in the AI, and their influence on behavioural outputs via the aMCC, might therefore suggest that the AI provides the emotional motivation behind reciprocal choices.

The ACC also boasts an extensive and wide-reaching connectivity profile. In addition to its connections with the insula cortex (Mufson & Mesulam, 1982), ACC projects to and receives input from lateral and orbital prefrontal cortex, temporolimbic structures and sensorimotor cortices (Vogt, Pandya, & Rosene, 1987). Given this diffuse connectivity profile, the ACC is considered a brain hub through which signals of emotional and motivational states are combined and translated into action (Apps et al., 2016). This converges with a wealth of research showing the engagement of ACC during cost–benefit evaluations that influence our motivation, and drive decisions to maintain or switch our current behaviour (Holroyd & Yeung, 2012; Kolling et al., 2016). For the sake of brevity, we have referred collectivity to the aMCC. Importantly, however, subdivisions exist within this cortical midline area, in terms of both cytoarchitecture and connectivity profiles; whilst both the gyrus and sulcus of the ACC connect with orbitofrontal cortex and the nucleus accumbens, indicating a shared processing of reward-related information to guide decision-making, the gyrus is connected more strongly with the superior temporal sulcus (Seltzer & Pandya, 1989) and temporal poles (Barbas, Ghashghaei, Dombrowski, & Rempel-Clower, 1999)—brain regions engaged during the inference of *others'* mental and intentional states. Furthermore, there is accumulating evidence from animal studies that the gyral aspect of the ACC processes the rewards for others (Chang, Gariépy, & Platt, 2013; Haroush & Williams, 2015), whereas the sulcus seems more sensitive to first-person reward (for a review, see Apps et al., 2013, 2016). This has led to the proposal that the gyrus of the ACC

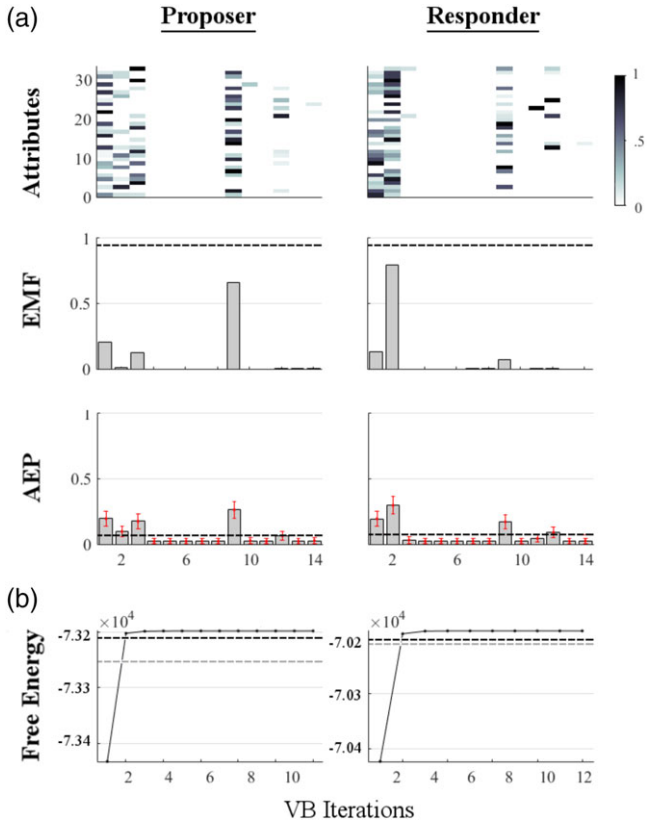

FIGURE 5 Results of variational Bayesian analysis. (a) Model attributes, expected model frequencies (EMFs) and approximated exceedance probabilities (AEPs) all converge to reveal that Models 9 and 2 emerged as the optimal models for Proposers and Responders, respectively. Model attributes are expressed as posterior probabilities for each model (*x* axis) to best explain each subject (*y* axis). For EMF, the dashed horizontal line shows the 'null' frequency profile over all models. (b) Variational Bayesian algorithm convergence. Free energy over VB iterations demonstrated that the observed log evidences are better explained by the random effects generative model than the fixed effects model or chance alone (black and grey dashed lines, respectively) [Color figure can be viewed at wileyonlinelibrary.com]

processes reward in an 'other-oriented' reference frame, which can be used to estimate the motivation and, in turn, predict the behaviour of others (Apps et al., 2016). Our aMCC node straddles both the right sulcus and gyrus of the aMCC. In this light, it is unsurprising to see brain responses within this region that are modulated by the perceived value of rewards distributed between the self and other, and the influence of the other's behaviour (motivation) on these valuations.

Due to their functional coupling and dense interconnectivity across a range of cognitive phenomena, the AI and ACC are believed to form a network that serves to motivate appropriate responses during social interactions. Both structures contain von Economo neurons (Allman et al., 2011), the wide axons of which will facilitate the speed of their integrative functions and the rapid transfer of information between them (see Craig, 2009). Through these connections, the representation of emotion states within AI can modulate the response-selection and decision-making processes of ACC (Medford & Critchley, 2010). Connectivity between the AI and ACC is also proposed to permit the generation of forward models of others' feeling states, allowing us to predict the behaviour of our interaction partners and respond accordingly (Bernhardt & Singer, 2012). Proposers must attempt such predictions of the Responder's behaviour over the multiple rounds of an iUG—in order to achieve some payout, they must propose divisions based upon the Responder's prior reactions. We provide evidence for the role of the AI–aMCC circuit in these predictions; our modelling shows that the strength of the connection from AI to aMCC in Responders is increased by estimates of EU from our reciprocity model. In other words, the more utility perceived in an offer, the stronger the connectivity between AI and aMCC and the more likely it is that the offer is accepted. It is also suggested that the reciprocal connectivity between these two brain regions allows for modulation in the reverse direction; ACC can project back onto AI to modulate the feeling state elicited by an input, and the modulated feeling state can then be sent forward to ACC for a more appropriate response selection (Medford & Critchley, 2010). We observed this feedback connection in both players, but in Proposers, it was modulated by round-by-round estimates of EU—that is, their valuation of a generous division in response to the Responder's prior behaviour. This suggests that the reciprocal decision to offer a generous division attenuates any further affective modulation.

This study presents the first application of bDCM to elucidate the patterns of effective connectivity behind the choices made during social interaction. Although our results demonstrate the huge potential of this technique to offer valuable insights into the brain connectivity behind social decision-making, they presents only a first step in understanding brain–behaviour relationships in interactive contexts. The complex and non-linear nature of bidirectional reciprocity likely involves much more elaborate and diffuse brain networks than the simple two-node circuit we have evaluated. In addition to the AI and aMCC, existing research into the brain connectivity associated with fairness evaluations (Feng et al., 2018; see also Feng et al., 2016) and reciprocal choices (Cáceda et al., 2015) has demonstrated the co-ordinated involvement of dorsomedial and ventromedial prefrontal cortex, the frontal pole and superior temporal sulcus during social decision-making.

This study has not considered player characteristics that might contribute towards individual differences in reciprocal tendencies and/or the underlying pattern of neural connectivity. For example, although we found no influence of age on brain responses modulated parametrically by our estimate of EU, a recent study reported that participants' age contributed to the degree of variability in their expressions of reciprocity beyond the strength of resting-state connectivity (Cáceda et al., 2015). More recently, knowledge about an opponent's socioeconomic status has been found to influence both behavioural and brain responses to unfairness during the UG (Zheng et al., 2017). Furthermore, although no direct associations have been found between personality dimensions and expressions of reciprocity in other forms of social exchange (Cáceda et al., 2017), they may influence an individual's affective response to an opponent's behaviour. Indeed, our exploratory analyses suggest that an individual's capacity for emotion regulation and their empathic expression might mediate the decision to reciprocate positively or negatively, thereby altering patterns of underlying brain connectivity. It has also been shown that certain socio-cognitive processes (e.g., mentalising) are involved in the

TABLE 3 Estimated model parameters from behavioural Dynamic Causal Modelling

Player	Model	AEP	EMF	BFP (±*SD*)
Proposer	1	0.20	27.78	72.63 (9.47)
	2	0.01	13.88	71.21 (10.42)
	3	0.13	24.92	71.41 (9.57)
	4	>0.01	3.05	70.81 (10.15)
	5	>0.01	3.07	71.47 (10.42)
	6	>0.01	3.08	72.58 (9.71)
	7	>0.01	3.22	71.31 (9.48)
	8	>0.01	3.10	71.72 (10.18)
	9	**0.66**	**37.44**	**71.45 (9.22)**
	10	>0.01	3.80	71.31 (9.59)
	11	>0.01	3.08	71.26 (10.10)
	12	>0.01	9.15	70.35 (10.61)
	13	>0.01	3.04	69.50 (9.98)
	14	>0.01	3.82	69.50 (9.98)
Responder	1	0.13	27.57	83.74 (11.28)
	2	**0.79**	**42.27**	**84.25 (11.01)**
	3	>0.01	4.467	83.91 (12.06)
	4	>0.01	3.06	83.79 (10.79)
	5	>0.01	3.10	83.10 (11.07)
	6	>0.01	3.10	82.87 (11.63)
	7	>0.01	3.17	83.74 (11.12)
	8	>0.01	3.15	82.93 (12.24)
	9	0.08	24.26	82.47 (12.22)
	10	>0.01	3.05	83.68 (11.53)
	11	>0.01	6.10	83.28 (11.02)
	12	>0.01	12.63	82.93 (12.24)
	13	>0.01	3.04	80.86 (12.35)
	14	>0.01	3.47	80.86 (12.35)

AEP = approximated exceedance probability; EMF = estimated model frequency; BFP = behavioural fit precision; *Note.* The bold values of models 9 (Proposers) and 2 (Responders) highlight the parameters of these winning models. The AEP and EMF indices correspond to those illustrated in Figure 1. The BFP values (mean [±SD]) represent the percentage of matches between real/observed player choices and those estimated by the behavioural Dynamic Causal Modelling procedure.

decision to reciprocate against norm violations (see Feng et al., 2016), and future research is needed to determine the potentially mediating influence of these factors on behavioural and neural indices of reciprocity. Finally, by examining reciprocity only among dyads of healthy males, the generalisability of our results is limited. Future research should investigate whether our findings extend to social interactions between female and mixed-sex dyads.

5 | CONCLUSION

This study introduces bDCM for research into social decision-making. Using this novel input-state-output modelling procedure, we have shown for the first time that specific patterns of neural dynamics between the right AI and aMCC drive decision-making during real-world social interaction. Behaviour over a series of economic exchanges was captured accurately by modelling choices in terms of EU influenced by reciprocity—that is, the degree to which players' valuations of payoff were influenced by the prior behaviour of their interaction partner. We then estimated player choices with over 70% accuracy by modelling effective connectivity between just these two brain regions. As such, our results provide evidence for the role of this network in high-level social cognition; the AI and aMCC work in tandem to guide social decisions on the basis of immediate and prior distributions of self-reward and other reward.

ACKNOWLEDGMENTS

This work was supported financially by project GA16-18261S. The authors would like to acknowledge the core facility CF MAFIL supported by the Czech-BioImaging large RI project (LM2015062 funded by MEYS CR) for their support with obtaining scientific data presented in this article.

CONFLICT OF INTEREST

The authors declare no competing financial interests.

ORCID

Daniel Shaw https://orcid.org/0000-0003-1139-8301

REFERENCES

Allman, J. M., Tetreault, N. A., Hakeem, A. Y., Manaye, K. F., Semendeferi, K., Erwin, J. M., … Hof, P. R. (2011). The von Economo neurons in the frontoinsular and anterior cingulate cortex. *Annals of the New York Academy of Sciences*, *1225*(1), 59–71. https://doi.org/10.1111/j.1749-6632.2011.06011.x

Apps, M. A. J., Lockwood, P. L., & Balsters, J. H. (2013). The role of the midcingulate cortex in monitoring others' decisions. *Frontiers in Neuroscience*, *7*, 251. https://doi.org/10.3389/fnins.2013.00251

Apps, M. A. J., Rushworth, M. F. S., & Chang, S. W. C. (2016). The anterior cingulate gyrus and social cognition: Tracking the motivation of others. *Neuron*, *90*(4), 692–707. https://doi.org/10.1016/j.neuron.2016.04.018

Augustine, J. R. (1996). Circuitry and functional aspects of the insular lobe in primates including humans. *Brain Research Reviews*, *22*(3), 229–244. https://doi.org/10.1016/S0165-0173(96)00011-2

Avrahami, J., Güth, W., Hertwig, R., Kareev, Y., & Otsubo, H. (2013). Learning (not) to yield: An experimental study of evolving ultimatum game behavior. *Journal of Socio-Economics*, *47*, 47–54. https://doi.org/10.1016/j.socec.2013.08.009

Barbas, H., Ghashghaei, H., Dombrowski, S. M., & Rempel-Clower, N. L. (1999). Medial prefrontal cortices are unified by common connections with superior temporal cortices and distinguished by input from memory-related areas in the rhesus monkey. *Journal of Comparative Neurology*, *410*(3), 343–367. https://doi.org/10.1002/(SICI)1096-9861(19990802)410:3<343::AID-CNE1>3.0.CO;2-1

Bernhardt, B. C., & Singer, T. (2012). The neural basis of empathy. *Annual Review of Neuroscience*, *35*(1), 1–23. https://doi.org/10.1146/annurev-neuro-062111-150536

Billeke, P., Zamorano, F., Cosmelli, D., & Aboitiz, F. (2013). Oscillatory brain activity correlates with risk perception and predicts social decisions. *Cerebral Cortex (New York, N.Y. : 1991)*, *23*(12), 2872–2883. https://doi.org/10.1093/cercor/bhs269

Billeke, P., Zamorano, F., López, T., Rodriguez, C., Cosmelli, D., & Aboitiz, F. (2014). Someone has to give in: Theta oscillations correlate with adaptive behavior in social bargaining. *Social Cognitive and Affective Neuroscience*, *9*(12), 2041–2048. https://doi.org/10.1093/scan/nsu012

Bolton, B. G. E., & Ockenfels, A. (2000). ERC: A theory of equity, reciprocity, and competition, The American Economic Review, American Economic Association, Vol. 90(1), 166–193. https://doi.org/10.1007/sl

Cáceda, R., James, G. A., Gutman, D. A., & Kilts, C. D. (2015). Organization of intrinsic functional brain connectivity predicts decisions to reciprocate social behavior. *Behavioural Brain Research*, *292*, 478–483. https://doi.org/10.1016/j.bbr.2015.07.008

Cáceda, R., Prendes-Alvarez, S., Hsu, J. J., Tripathi, S. P., Kilts, C. D., & James, G. A. (2017). The neural correlates of reciprocity are sensitive to prior experience of reciprocity. *Behavioural Brain Research*, *332*, 136–144. https://doi.org/10.1016/j.bbr.2017.05.030

Chang, S. W., Gariépy, J. F., & Platt, M. L. (2013). Neuronal reference frames for social decisions in primate frontal cortex. *Nature Neuroscience*, *16*(2), 243–250. https://doi.org/10.1038/nn.3287.Neuronal

Charness, G., & Rabin, M. (2002). Understanding social preferences with simple tests. *Quarterly Journal of Economics*, *117*(3), 817–869.

Cox, J. C., Friedman, D., & Gjerstad, S. (2007). A tractable model of reciprocity and fairness. *Games and Economic Behavior*, *59*(1), 17–45. https://doi.org/10.1016/j.geb.2006.05.001

Craig, A. D. (2009). How do you feel--now? The anterior insula and human awareness. *Nature Reviews. Neuroscience*, *10*(1), 59–70. https://doi.org/10.1038/nrn2555

Daunizeau, J., Adam, V., & Rigoux, L. (2014). VBA: A probabilistic treatment of nonlinear models for neurobiological and behavioural data. *PLoS Computational Biology*, *10*(1), e1003441. https://doi.org/10.1371/journal.pcbi.1003441

Davis, M. H. (1983). Measuring individual differences in empathy: Evidence for a multidimensional approach. *Journal of Personality and Social Psychology*, *44*(1), 113–126.

Erev, B. I., & Roth, A. E. (1998). Predicting how people play games: Reinforcement learning in experimental games with unique, mixed strategy equilibria. *The American Economic Review*, *88*(4), 848–881.

Falk, A., & Fischbacher, U. (2006). A theory of reciprocity. *Games and Economic Behavior*, *54*(2), 293–315.

Fehr, E., & Schmidt, K. M. (1999). A theory of fairness, competition, and cooperation. *Quarterly Journal of Economics*, *114*(3), 817–868.

Feng, C., Deshpande, G., Liu, C., Gu, R., Luo, Y. J., & Krueger, F. (2016). Diffusion of responsibility attenuates altruistic punishment: A functional magnetic resonance imaging effective connectivity study. *Human Brain Mapping*, *37*(2), 663–677. https://doi.org/10.1002/hbm.23057

Feng, C., Feng, X., Wang, L., Wang, L., Gu, R., Ni, A., … Luo, Y. J. (2018). The neural signatures of egocentric bias in normative decision-making. *Brain Imaging and Behavior*, https://doi.org/10.1007/s11682-018-9893-1

Feng, C., Luo, Y. J., & Krueger, F. (2015). Neural signatures of fairness-related normative decision-making in the ultimatum game: A coordinate-based meta-analysis. *Human Brain Mapping*, *36*(2), 591–602. https://doi.org/10.1002/hbm.22649

Friston, K. J., Harrison, L., & Penny, W. (2003). Dynamic causal modelling. *NeuroImage*, *19*(4), 1273–1302. https://doi.org/10.1016/S1053-8119(03)00202-7

Gabay, A. S., Radua, J., Kempton, M. J., & Mehta, M. A. (2014). The ultimatum game and the brain: A meta-analysis of neuroimaging studies. *Neuroscience and Biobehavioral Reviews*, *47*, 549–558. https://doi.org/10.1016/j.neubiorev.2014.10.014

Gajdoš, M., Mikl, M., & Mareček, R. (2016). Mask_explorer: A tool for exploring brain masks in fMRI group analysis. *Computer Methods and Programs in Biomedicine*, *134*, 155–163. https://doi.org/10.1016/j.cmpb.2016.07.015

Güth, W., Schmittberger, R., & Schwarze, B. (1982). An experimental analysis of ultimatum bargaining. *Journal of Economic Behavior and Organization*, *3*(4), 367–388. https://doi.org/10.1016/0167-2681(82)90011-7

Haroush, K., & Williams, Z. M. (2015). Neuronal prediction of opponent's behavior during cooperative social interchange in primates. *Cell*, *160*(6), 1233–1245. https://doi.org/10.1016/j.cell.2015.01.045

Hasson, U., & Frith, C. D. (2016). Mirroring and beyond: coupled dynamics as a generalized framework for modelling social interactions. *Philosophical Transactions of The Royal Society B Biological Sciences*, *371*(1693), 20150366. https://doi.org/10.1098/rstb.2015.0366

Henrich, J., Ensminger, J., Bowles, S., Gil-white, F., Fehr, E., Marlowe, F. W., & Patton, J. Q. (2005). Economic man in cross-cultural perspective: Behavioral experiments in 15 small-scale societies. *Behavioral and Brain Sciences*, *28*, 795–855.

Holroyd, C. B., & Yeung, N. (2012). Motivation of extended behaviors by anterior cingulate cortex. *Trends in Cognitive Sciences*, *16*(2), 122–128. https://doi.org/10.1016/j.tics.2011.12.008

Johnson, E. J., Camerer, C., & Rymon, T. (2002). Detecting Failures of Backward Induction: Monitoring Information Search in Sequential Bargaining 1. *Journal of Economic Theory*, *104*, 16–47. https://doi.org/10.1006/jeth.2001.2850

Kelly, C., Toro, R., Di Martino, A., Cox, C. L., Bellec, P., Castellanos, F. X., & Milham, M. P. (2012). A convergent functional architecture of the insula emerges across imaging modalities. *NeuroImage*, *61*(4), 1129–1142. https://doi.org/10.1016/j.neuroimage.2012.03.021

Kolling, N., Wittmann, M. K., Behrens, T. E. J., Boorman, E. D., Mars, R. B., & Rushworth, M. F. S. (2016). Value, search, persistence and model updating in anterior cingulate cortex. *Nature Neuroscience*, *19*(10), 1280–1285. https://doi.org/10.1038/nn.4382

Krueger, F., Grafman, J., & McCabe, K. (2008). Neural correlates of economic game playing. *Philosophical Transactions of the Royal Society B: Biological Sciences*, *363*(1511), 3859–3874. https://doi.org/10.1098/rstb.2008.0165

Kuhl, J. (1994). Action versus state orientation: Psychometric properties of the Action Control Scale (ACS-90). In J. Kuhl & J. Beckmann (Eds.), *Volition and personality: Action versus state orientation* (pp. 47–56). Seattle, WA: Hogrefe Huber.

Kurth, F., Zilles, K., Fox, P. T., Laird, A. R., & Eickhoff, S. B. (2010). A link between the systems: Functional differentiation and integration within the human insula revealed by meta-analysis. *Brain Structure and Function*, *214*(5–6), 519–534. https://doi.org/10.1007/s00429-010-0255-z

Mailath, G. J., & Samuelson, L. (2006). *Repeated games and reputations: Long-run relationships*. New York, NY: Oxford University Press.

Medford, N., & Critchley, H. D. (2010). Conjoint activity of anterior insular and anterior cingulate cortex: Awareness and response. *Brain Structure and Function*, *214*(5–6), 535–549. https://doi.org/10.1007/s00429-010-0265-x

Mesulam, M. M., & Mufson, E. J. (1982a). Insula of the old world monkey. III: Efferent cortical output and comments on function. *Journal of Comparative Neurology*, *212*(1), 38–52. https://doi.org/10.1002/cne.902120104

Mesulam, M. M., & Mufson, E. J. (1982b). Insula of the old world monkey. Architectonics in the insulo-orbito-temporal component of the paralimbic brain. *The Journal of Comparative Neurology*, *22*(1), 1–22.

Mufson, E. J., & Mesulam, M. (1982). Insula of the old world monkey. II: Afferent cortical input and comments on the claustrum. *Journal of Comparative Neurology*, *212*(1), 23–37.

Namkung, H., Kim, S. H., & Sawa, A. (2017). The insula: An underestimated brain area in clinical neuroscience, psychiatry, and neurology. *Trends in Neurosciences*, *40*(4), 200–207. https://doi.org/10.1016/j.tins.2017.02.002

Penny, W. D., Stephan, K. E., Mechelli, A., & Friston, K. J. (2004). Comparing dynamic causal models. *NeuroImage*, *22*(3), 1157–1172. https://doi.org/10.1016/j.neuroimage.2004.03.026

Rigoux, L., & Daunizeau, J. (2015). NeuroImage dynamic causal modelling of brain – Behaviour relationships. *NeuroImage*, *117*, 202–221. https://doi.org/10.1016/j.neuroimage.2015.05.041

Rigoux, L., Stephan, K. E., Friston, K. J., & Daunizeau, J. (2014). Bayesian model selection for group studies - Revisited. *NeuroImage*, *84*, 971–985. https://doi.org/10.1016/j.neuroimage.2013.08.065

Rilling, J. K., & Sanfey, A. G. (2011). The neuroscience of social decision-making. *Current Opinion in Neurobiology*, *62*, 23–48. https://doi.org/10.1016/j.conb.2008.06.003

Seltzer, B., & Pandya, D. N. (1989). Frontal lobe connections of the superior temporal sulcus in the rhesus monkey. *Journal of Comparative Neurology*, *281*(1), 97–113.

Stephan, K. E., Harrison, L. M., Kiebel, S. J., David, O., Penny, W. D., & Friston, K. J. (2007). Dynamic causal models of neural system dynamics: Current state and future extensions. *Journal of Biosciences*, *32*(1), 129–144. https://doi.org/10.1007/s12038-007-0012-5

Stephan, K. E., Penny, W. D., Daunizeau, J., Moran, R. J., & Friston, K. J. (2009). Bayesian model selection for group studies. *NeuroImage*, *46*(4), 1004–1017. https://doi.org/10.1016/j.neuroimage.2009.03.025

Uddin, L. Q. (2015). Salience processing and insular cortical function and dysfunction. *Nature Reviews Neuroscience*, *16*(1), 55–61. https://doi.org/10.1038/nrn3857

van Damme, E., Binmore, K. G., Roth, A. E., Samuelson, L., Winter, E., Bolton, G. E., … Azar, O. H. (2014). How Werner Güth's ultimatum game shaped our understanding of social behavior. *Journal of Economic Behavior and Organization*, *108*, 292–318. https://doi.org/10.1016/j.jebo.2014.10.014

Vogt, B. A., Pandya, D. N., & Rosene, D. L. (1987). Cingulate cortex of the rhesus monkey: I. Cortical afferents. *The Journal of Comparative Neurology*, *262*(2), 271–289. https://doi.org/10.1002/cne.902620208

Wager, T. D., & Nichols, T. E. (2003). Optimization of experimental design in fMRI: A general framework using a genetic algorithm. *NeuroImage*, *18*(2), 293–309. https://doi.org/10.1016/S1053-8119(02)00046-0

Wang, G., Li, J., Li, Z., Wei, M., & Li, S. (2016). Medial frontal negativity reflects advantageous inequality aversion of proposers in the ultimatum game: An ERP study. *Brain Research*, *1639*, 38–46. https://doi.org/10.1016/j.brainres.2016.02.040

Zheng, Y., Cheng, X., Xu, J., Zheng, L., Li, L., Yang, G., & Guo, X. (2017). Proposers' economic status affects behavioral and neural responses to unfairness. *Frontiers in Psychology*, *8*, 1–8. https://doi.org/10.3389/fpsyg.2017.00847

SUPPORTING INFORMATION

Additional supporting information may be found online in the Supporting Information section at the end of the article.

How to cite this article: Shaw D, Czekóová K, Gajdoš M, Staněk R, Špalek J, Brázdil M. Social decision-making in the brain: Input-state-output modelling reveals patterns of effective connectivity underlying reciprocal choices. *Hum Brain Mapp*. 2018;1–14. https://doi.org/10.1002/hbm.24446